INTERNATIONAL ATOMIC ENERGY AGENCY
UNITED NATIONS EDUCATIONAL, SCIENTIFIC AND CULTURAL ORGANIZATION
INTERNATIONAL CENTRE FOR THEORETICAL PHYSICS
I.C.T.P., P.O. BOX 586, 34100 TRIESTE, ITALY, CABLE: CENTRATOM TRIESTE

SMR.379/43

COURSE ON BASIC TELECOMMUNICATIONS SCIENCE

9 January - 3 February 1989

"PROPAGATION IN THE ATMOSPHERE AND IONIZED MEDIA

DR. F. MOUPFOUMA
Avion Marcel Dassault
Breguet Aviation
Paris St. Cloud
FRANCE

PROPAGATION IN THE ATMOSPHERE AND IONIZED MEDIA

Dr. MOUPFOUMA Fidèle

Avion MARCEL DASSAULT BREGUET AVIATION
PARIS ST. CLOUD

PROPAGATION IN THE ATMOSPHERE AND IONIZED MEDIA

PROPAGATION IN THE ATMOSPHERE

A) - INTRODUCTION

The behaviour of communication systems depends on local climatology. The design and implementation of such systems involve an accurate knowledge of propagation parameters which govern link availability and service quality. Propagation abnormalities adversely affecting performances of communication systems in the atmosphere can be classified into clear air effects, and rain induced perturbations. For microwave systems operating at high frequencies, rain effects have long been recognized as a major limitation, mainly in tropical and equatorial areas.

B) RAIN EFFECTS ON TERRESTRIAL AND EARTH - SATELLITE TELECOMMUNICATION MICROWAVE SYSTEMS IN EQUATORIAL AND TROPICAL AREAS

The saturation of the frequency bands under 10 GHZ on which attention was focused during many international meetings on microwave communications during the late 1970s has led to use higher frequencies. The world Administration Conference (WARC) on frequency sharing which was held in geneva in 1979, allowed developed, as well as developing countries to share frequencies in order to plan their future radiocommunication networks using wideband microwave systems.

Unfortunately, as frequency increases, wavelength approaches the size of raindrops which, therefore, act as a screen of scatters for the wave. Rainfall occuring over the links affects transmission quality and thus limits the system's performances.

The magnitude of rain effects on microwave systems is due to several factors among which the rainfall rate cumulative distribution and raindrop spectrum characterising the rain structure in the concerned zone.

Rain effects on microwave systems are more critical in tropical and equatorial zones, where rainfall is higher than in temperate zones.

The aim of this section is a quantitative assessment of the influence of rainfall rate distribution and large drop, mainly on attenuation due to rain on earth-satellite or terrestrial microwave systems.

B - I- RAINFALL STRUCTURE

B - I - 1) Types of rainfalls

Two types of rainfalls are generally considered [1] viz :

- Convective rains (including local storms) characterized by strong showers with high rain rates. They result from atmospheric instability due to heat and moisture. Convective rains are generally observed in small areas for a short time period

Stratiform rains are characterized by medium and lower intensities. They can be observed for a long time period and may extend over very large areas. As a rule, rainfall varies in intensity, duration, and spatial pattern. The climatology is influenced by the surrounding geographical features such as water masses (oceans, great lakes...), mountains, hills, etc. Rainfall increases in duration as moist streams approach the crest lines of hill or mountain ranges, its patterns being complicated locally by the effects of spur valleys and terrain features

B - II- PARAMETERISATION OF RAINFALL RATE AS A FUNCTION OF DURATION

(Extract from [1])

When analysing rainfall rate data for propagation studies, one has on the one hand parameters R(mm/h) and T(hours), representing respectively the rain rate and the total duration of the propagation experiment, and on the other hand parameters t and p such that t represents the total time during the experiment for which the rain rate R is exceeded, and p represents this time as a percentage of the total duration of the test (T); i.e.

$$t = \sum_{i=1}^{n} \delta_{ti} \qquad (1)$$

$$p(\%) = \frac{t}{T} \times 100 \qquad (2)$$

Using rainfall rate cumulative distributions for regions representative both of temperate and tropical climatic zones, it appears that rain rates and their corresponding time percentages of exceedance may be roughly related through the following non linear relationship:

$$R\,(mm/h) = \frac{q}{P(\%)^{v}} \qquad (3)$$

B - II - 1) Behaviour of parameters q and v according to climatic zones

In the following, we only consider the percentage of time p(%) in a year for a given precipitation rate R(mm/h) to be exceeded. Using the data of table 1, values of parameters q and v which can verify equation 3 are :

(a) Temperate zones

Locations	q	v
Austin (USA)	7.04	0.42
Blacksburg (USA)	2.71	0.56
Clayton (Australia)	5.17	0.48
Darmstadt (FRG)	2.12	0.49
Gometz (France)	2.17	0.47
Kirkkonummi (FLN)	2.07	0.52
Lario (Italy)	3.68	0.53
Leeheim (FRG)	2.5	0.54
Mendlesham (UK)	1.48	0.53
Nederhorst (HOL)	3.23	0.45
Paris (France)	2.59	0.53

(b) Tropical zones

Locations	q	v
Belém (Brazil)	20.9	0.33
Danang (Vietnam)	22.3	0.3
Darwin (Australia)	26.32	0.32
Innisfail (Australia)	33.53	0.3
Djatiluhur (Indonesia)	31.35	0.25
Korhogo (Ivory Coast)	29.8	0.3
Manaus (Brazil)	21.5	0.3
PK 45 (Congo)	18.25	0.35
Saigon (Vietnam)	18.12	0.35

Inspection of these results shows that parameter q has higher values in tropical climatic zones than in temperate zones. Moreover these values vary quite considerably from one location to another in the same climatic zone. As far as parameter v is concerned, its values are different for the two categories of zones, and these values can be represented by their mean value , which is 0.5 for temperate zones, and 0.31 for tropical zones with a standart deviation value of about 10 % of the mean.

Table 1 : Rain rate cumulative distribution in some tropical and temperate locations

Time percentage	10^{-3}	3	10^{-2}	3	10^{-1}
Duration, min	5	16	53	158	526
(a) Temperate zones					
Austin (USA)	116	85	54	35	16
Blacksburg (USA)	104	74	43	21	8
Clayton (Australia)	115.5	82.5	54	35.5	16.5
Darmstadt (FRG)	50	38	22	12	5.5
Gometz (France)	54	35	21	11.5	6
Kirkkonummi (FLN)	64	37.9	23	13	6.4
Lario (Italy)	117	84	52	27.8	12.5
Leeheim (FRG)	83	66.1	33	17.8	7.4
Mendlesham (UK)	50	32	18	10	4.5
Nederhorst (HOL)	66	47	30	17.2	8
Paris (France)	90	58	33	17	6
(b) Tropical zones					
Belém (Brazil)	190	150	100	75	40
Danang (Vietnam)	150	125	90	64	40
Darwin (Australia)	215	178	130	86	49
Innisfail (Australia)	229	189	142	107	70
Djatiluhur (Indonesia)	162.8	138.5	109.2	79.2	51
Korhogo (Ivory Coast)	222	172	122	90	55
Manaus (Brazil)	140	130	88	65	40
PK 45 (Congo)	183	145	105	70	35
Saigon (Vietnam)	195	150	110	70	36

This accuracy is relative to the error of rainfall rate measurements, and v is obviously a climate dependent parameter. So, as pointed out under, it may be concluded that in temperate zones, rainfall rate is approximately proportional to reciprocal of the square root of time percentage, while in tropical zones it is roughly proportional to the inverse cubic root of the time percentage.

Temperate zones

$$R\,(mm/h) \quad a \quad \frac{1}{\sqrt{P(\%)}}$$

Tropical zones

$$R\,(mm/h) \quad a \quad \frac{1}{P(\%)^{0.3}}$$

Parameter v has smaller values in tropical zones than in temperate zones, because in the first case precipitations are due to squal lines and convective rains, which give rise to high rainfall intensities already mentioned as having a short duration. In the second case rainfall intensities are due to stratiform precipitations, which are of long duration.

A thorough study of parameter q should take into consideration the local rain characteristics: Size of rain cells, type of clouds and rains, etc. Moreover, the knowledge of a mathematical relationship giving parameter q according to climates could allow a rain rate cumulative prediction law to be determined. However this study of parameter q is out of the scope of this paper, and we will study the prediction of rain rate cumulative distribution in another way.

B - III- Measurement of rainfall rate data

To obtain rainfall rate data in a place where radiocommunication systems have to be implemented, one can :

a) use the data collected during many years in various places by national meteorological administrations. However the aim of these administrations is not to study radiowave propagation, and the integration time they use for collecting their data is too long (1 hour or even more) for the radio system designs, and unfortunately conversion laws which allow determination of instantaneous rain rates with a given integration time cannot be safely used.

b) carry out rainfall rate measurements by means of raingauges with small resolution time (from a few seconds to 6 minutes). These allow the instantaneous local rainfall rate to be determined and therefore well suited for radio engineering. The use of several spaced raingauges allows the spatial extend of the rain and the cell sizes to be accounted for. Moreover, the longer the duration of such data collecting, the more significant the results are. The use of radar or satellite measurements, which are expensive techniques, allows more informations on the rain structure (rain cells, etc.) to be gathered, but rainfall intensities derived from such measurements are not accurate enough for radio system designers.

B - IV -Estimations of instantaneous rain rates

As pointed out in the introduction, CCIR has developed in its report 563-3, two world wide maps, one with contours of rainfall intensity $R_{0.01}$ (mm/h) exceeded for 0.01% of the time , another giving rain climatic zones which divide the world into several areas of unequal rainfall intensities [2]. Contours of $R_{0.01}$ (mm/h) are well defined, mainly for temperate zones, but unfortunately they are incomplete, and isopleths for other percentages of time are useful. CCIR rain climatic zones cover almost all the world, however, they are not precise enough. It is necessary to have a mathematical or empirical model which correctly models rain rate cumulative distributions whatever the climatic zone.

Many prediction models have been proposed, in particular the Log-normal and the Gamma law, the Rice - Holmberg model and that of Dutton and Dougherty. The first two are well known. Log-normal is appropriate for low and medium rainfall rates, while the Gamma model gives a good representation of medium and high rain rates. However, none of them is globaly applicable to different hydrometeorological zones. These asymptotical distributions merge at about 20 to 50 mm/h (depending on the climate), which is sometimes troublesome for applications, since it corresponds to a value which is of a great importance [3].

The analysis of rainfall rate data collected during a radiowave propagation experiment, which lasted more than two years, in Brazzaville (Congo) led the author to propose an experimental probability law which allows us to represent all rainfall cumulative distributions by a single function in the whole range of useful values.

If rainfall rate values greater than 2 mm/h are considered, this function has the following form [3]:

$$P(R \geq r) = a \frac{e^{-ur}}{r^b} \qquad r \geq 2\ mm/h \tag{4}$$

with parameters a, b, u depending on the integration time of the raingauges used as well as on the geographical characteristics of the locality of interest.

F(r) being the distribution function which characterizes the random variable r(mm/h) as

$$F(r) = P(R < r) = 1 - P(R \geq r) \tag{5}$$

the probability density associated with equation 4 is

$$f(r) = \frac{dF}{dr} = \begin{cases} \dfrac{a}{r^b}\left(u + \dfrac{b}{r}\right) exp(-ur) & r(mm/h) > 0 \\ 0 & r(mm/h) \leq 0 \end{cases} \tag{6}$$

Since $F(+\infty) = 1$, u is always positive, and b can be restricted to positive values. Moreover $P(R \geq r)$ must be smaller or equal to 1. This condition is not generally thrue since $P(R \geq r)$ takes an infinite value when r is zero. However, if we assume that in practice $r \geq 2$ mm/h, the condition is in fact always satisfied with $0 < a < 1$ as shown in reference [3].

B - V Evaluation of parameters of the model.

In a previous paper [3,4], using rainfall data from a number of hydrometeorological zones, the author has shown that parameters a and b in equation 4 are related to the rainfall intensity $R_{0.01}$ (mm/h) exceeded for 0.01 % of the time for any integration time as follows

$$a = 10^{-4} R_{0.01}^{\,b} \exp(u R_{0.01}) \qquad (7)$$

$$b = 8.22 R_{0.01}^{-0.584} \qquad (8)$$

Equation 4 may then be written as.

$$P(R \geq r) = 10^{-4} \left(\frac{R_{0.01}}{r}\right)^{b} \exp\left(ur\left(\frac{R_{0.01}}{r} - 1\right)\right) \qquad (9-a)$$

$$b = 8.22 R_{0.01}^{-0.584} \qquad (9-b)$$

The model then becomes dependent on

(a) $R_{0.01}$ (mm/) which accounts for the shape of the distribution

(b) u which describes the slope of the curve.

When both these parameters are known, equation 9 gives rainfall cumulative distribution for any locality. The use of $R_{0.01}$ as a parameter in our model is helpful since its values are known with great precision from CCIR data base. Fitting of data shows that for $u = 2.5 \times 10^{-2}$, the model gives a good representation of instantaneous rainfall rate for a great number of localities across the world [1].

However, in some countries, such as Japan, climatic and geographical features (mountains, great extents of water, etc) prevent the use of this value of parameter u.To have a better fit of rain cumulative distributions from as many localities across the world as possible, we propose two variants of the above model, the first with u as a function of rain rate, and the second one with u values given in table 4. For the first variant, u is derived from the cumulative distributions representing the CCIR rain climatic zones. For the second Variant of the method, values of u are calculated from data collected in 162 localities across the world, and depend on the climate and geographical features.

B - V-1 First variant of the method: rain climatic zone dependant parameter λ, s

Let us analyse the rain climatic zones proposed by CCIR (Table 2). Their inspection shows that only zones D to P are of interest for rain studies, since zones A, B, and C are scarcely rainy, being either desert or covered with ice.

Moreover, most of available experimental rain data in the CCIR data base or in the literature have been gathered in places located within this first group of zones [5], nevertheless using the rain distributions characterising those zones, we noticed that they did not give a good fit when using a constant value of parameter u in the formulas. To improve the model, we considered u as a function of the rain rate, and expressed it as :

$$u = \lambda r^{-s} \qquad (10)$$

where λ and s are parameters derived, for each climatic zone, from data table 2 and are listed in table 3 and r(mm/h) is the rain rate characterising a given zone.

Table 2 : CCIR rain climatic zones [7] rainfall intensity exceeded (mm/h)

Percentage of time	A	B	C	D	E	F	G	H	J	K	L	M	N	P
1.0	-	1	-	3	1	2	-	-	-	2	-	4	5	12
0.3	1	2	3	5	3	4	7	4	13	6	7	11	15	34
0.1	2	3	5	8	6	8	12	10	20	12	15	22	35	65
0.03	5	6	9	13	12	15	20	18	28	23	33	40	65	105
0.01	8	12	15	19	22	28	30	32	35	42	60	63	95	145
0.003	14	21	26	29	41	54	45	55	45	70	105	95	140	200
0.001	22	32	42	42	70	78	65	83	55	100	150	120	180	250

Table 3 : Values of parameters λ and s according to CCIR climatic zones

	D	E	F	G	H	J	K	L	M	N	P
λ	0.18	0.05	0.07	0.14	0.06	0.07	0.05	0.05	0.05	0.033	0.035
s	0.33	0.29	0.32	0.28	0.19	0.18	0.17	0.22	0.09	0.06	0.1

As an example, suitable values of u calculed for CCIR climatic zone L from eqn 9 and listed in Table 3 are approximated for CCIR climatic zone L by :

$$u = 0.05 r^{-0.22} \qquad (11)$$

Table 4: Parameter u values versus rain rate in climatic zone L

R (mm/h)	150	105	60	33	17	7
u	0.017	0.0174	0.022	0.024	0.027	0.032

Thus provided that the correct CCIR climatic zone has been chosen, and that $R_{0.01}$ (mm/h) value for the concerned locality is known, the rainfall rate cumulative distribution

$$P(R \geq r) = 10^{-6}\left(\frac{R_{0.01}}{r}\right)^{b} \exp\left(\lambda r^{1-c}\left(\frac{R_{0.01}}{r} - 1\right)\right) \qquad (12-a)$$

$$b = 8.22\, R_{0.01}^{-0.584} \qquad (12-b)$$

may be predicted from eqn. 12 and Table 2. Fig 1 shows a comparison between predicted results with experimental data gathered in Belém (Brazil) and Darwin (Australia) which belong in the CCIR zone P, while Fig. 2 relates to Dijon (France) and Madrid (Spain) which are located within zone H. A good agreement is achieved as shown in the two figures.

CCIR rain climatic zones cover nearly all the world; unfortunately they seem to be too roughly determined for local climatic effects in some regions necessarily to be taken into account. So the model given by eqn. 12 might not provide an accurate representation of rain rate whatever the locality. To take into account the influence of geographical features on nearby climatology, we propose a second variant of the method given by eqn. 9, now using values of parameter u calculated from data collected at 162 sites of which 4 are in Africa, 60 in America, 30 in Asia, 27 in Australia, 40 in Europe and 1 in the Middle East. Since for time percentages less than 0.001% rainfall intensities are very high and affected by substantial errors, and at over 1% of the time, attenuations observed on radio links are no longer related to rain rates, we have calculated the values of parameter u for rain rates corresponding to time percentages ranging from 1% to 0.001% [1]

B - V - 2 Second variant of the method : parameter u dependent on climate and geographical features.

The use of the model given by eqn. 9 for any locality requires the knowledge of both $R_{0.01}$ and u values for the concerned locality. Due to geographical nonuniformity such as the presence of mountain or great extents of water (oceans, lakes,...) parameter u has been determined for 162 localities across the world (among which 4 Africa,60 in America, 30 in Asia, 27 in Australia, 40 in Europe 1 in the Middle East) for rain rates corresponding to time precentages ranging from 1% to 0.001%. Moreover, the dependency of parameter u on climate and geographical characteristics of those localities has been investigated [4,1,5].

When evaluating "u", it has been noticed that :

- localities near extents of water or mountains are characterized by high values of "u", with flatter distributions, due to the predominance of stratiform rainfalls.

- continental areas are characterized by low values of "u" with steeper distributions due to the predominance of convective rainfalls.

Table 5 gives values of parameter u which depend on the climate and geographical features

Localities	Temperates zones					Tropical zones
Localities near extents of water or mountains. Coastal areas	Europe		American		Japan	
	Central southern	Northern	Canada	USA		
	0.03	0.045	0.032	0.032	0.045	0.042
Average rolling terrain	0.025	0.025	0.025	0.025	0.045	0.025
Arid regions			0.015	0.015		

Table 5

B - VI - Choice of prediction method according to conditions

In section V, we showed that due to its flexibility, our empirical model is suited to the prediction of rainfall intensity, provided that $R_{0.01}$ and u are known.

According to an overall picture of the world climatic situation, tropical climates are more uniform than temperate ones, which might explain why in table 2 (from CCIR) only zones N and P are necessary to represent all tropical climates, although temperate ones are represented by several different zones such as M, L, K, J, H, G, F, E, etc. Nethertheless, more rainfall data from tropical regions should provide a better delimitation of CCIR tropical rain climatic zones, mainly on the coastal areas.

Eventually, both the first and the second variants of the model can safely be used (see fig 3 and 4). Nevetheless, for localities for which there are no more data (mainly tropical ones), the use of the first variant of the model, given by equation 12 and table 3 is recommanded, whilst in the other cases - mainly in localities close to large extents of water or mountains, localities prone to micro climates - one has to use the second variant,given by eqns.9 together with parameter u values given in Table 5.

B - VII- Limitations of the proposed law

Our prediction method relies on the values of parameters u and $R_{0.01}$ (mm/h). Its use suffers from some limitations due to two sources of errors :

(i) *Statistical limits on data* :

compared to occurences of medium rainfall rates, the number of the highest rainfall events (above 120 mm/h) is sometimes not significant. This generally leads to a steep change in the slope of the distribution curve, while on the other hand low rain rates present a high annual number of occurences, but they offer little contribution to the determination of rain cumulative distribution.

(ii) *Measurement errors* :

the accuracy of data is related to that of recorders. Leaves can block the raingauge, sand or dust can accumulate in the gauge and can become mud in the buckets, disturbing their swinging motions, and so on. All these factors reduce measurement accury. Saturation of a raingauge induces a bias to the measurements of high rain rates, and mechanical limitations reduce the accuracy of the measurements. Also, the lack of sensitivity of some raingauge leads to errors in low rain rates. These errors of the collected data of course have an effect on the evaluation of parameter u.

In conclusion rainfall rate data are needed for the design of radiocommunication systems. In this paper, two variants of an empirical model allowing the calculation of 1 minute point rain rate cumulative distribution are proposed.

(i) $R_{0.01}$ (mm/h) represents the rainfall exceeded for 0.01% of the time in the considered location, and may be obtained by using CCIR contour curves. It describes the shape of the cumulative distribution.

(ii) Parameter u characterises the slope of this cumulative distribution, and its values can be obtained in two different ways :

$u = \lambda r^s$ is recommended provided that the zone to which the site of interest belongs is well known. λ and s are dependent of climatic zones and are listed in table 3

For islands, or cities located in the vicinity of large masses of water such as oceans, great lakes, large rivers or hilly regions, the use of eqns. 9 along with the values of parameter u given in Table 5 should give better results.

Fig.1 Comparison between measured and predicted rain data : a- *Darwin* (Australia); b-*Bélem*(Brazil)

Fig.2 Comparison between measured and predicted rain data : a- *Dijon (France)*; b-*Madrid (Spain)*

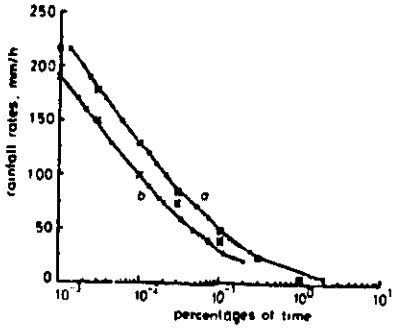

Fig. 1 *Comparison between measured and predicted rain data in Darwin (Australia) and Belem (Brazil)*

a Darwin × measured + $\lambda = 0.033$; $s = 0.1$ b Belém × measured + $\lambda = 0.035$; $s = 0.1$

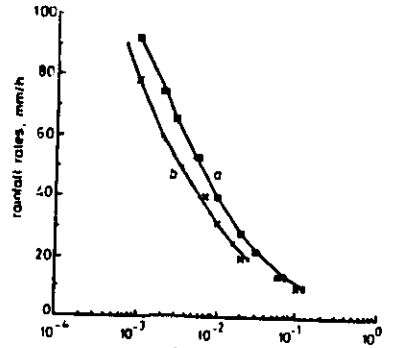

Fig. 2 *Comparison between measured and predicted rain data in Dijon (France) and Madrid (Spain)*

a Dijon × measured ◆ $\lambda = 0.08$; $s = 0.19$ b Madrid × measured + $\lambda = 0.06$; $s = 0.19$

Fig.3 Comparison between measured and predicted rain data from the 2 variant of model : *Holmdel (USA)*.

Fig.4 Comparison between measured and predicted rain data from the 2 variant of model: *Pk-45 (Congo)*

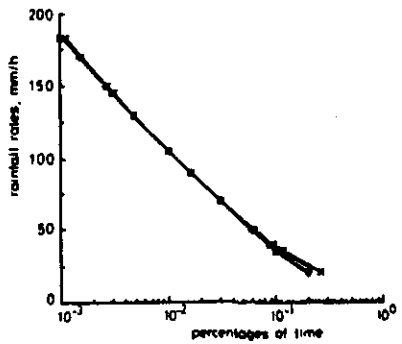

Fig. *Comparison between measured and predicted rain data obtained from the two variants of the model at PK-45 (Congo)*

PK-45 (Congo) ⊡ measured ◆ $s = (0.025, 0.025)$ $\lambda = 0.033$, $s = 0.06$

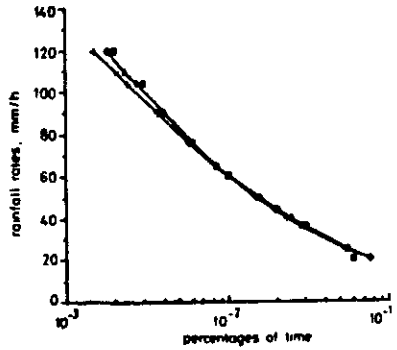

Fig. *Comparison between measured and predicted rain data obtained from the two variants of the model in Holmdel (USA)*

Holmdel ⊡ measured ◆ $s = (0.02, 0.03)$ + $\lambda = 0.05$, $s = 0.17$

C - Rainfall rate behaviour versus drop size.

The raindrop spectrum is the basic data for evaluating the attenuation of electromagnetic radiation over a given path through rain.

Convective rains (heavy rains) are generally characterized by large raindrops, while stratiform rains are governed by mean and small raindrops.

While small,raindrops are spherical, when falling towards the ground due the process of coalescence they become large; moreover, due to gravitational and electrical forces, along with thrust, they become oblate or prolate spheroïds.[5]

1) - Radiowave scattering by raindrops

The study of rain effects on microwave systems requires an understanding of the scattering theory of electromagnetic waves by raindrops.

The basis is the general theory of scattering by a sphere. Many brillant physicists worked on this topic using *Maxwell* electromagnetic theory *(Rayleigh 1881) and (Mie 1908), Debye* (1909).[5].

Various treatments of this theory may be found in *Stratton (5),Van de Hulst [5] Kerker* [5].

Even if large raindrops are rather oblate let us assume that they can be considered spheroïdal with "a" as equivolumetric radius.

Whenever a plane wave is incident upon a spherical particle possessing optical constants different from those of the medium, a scattered wave is generated.

The field vectors describing the electromagnetic properties of space may be resolved into three parts :

- the incident wave E_i H_i;
- the wave inside the particule E_r H_r;
- the scattered wave E_s H_s.

Let us consider a spherical particle in an infinite homogeneous medium. This isotropic homogeneores sphere is characterized by a propagation constant k_1, While k_2 is the propagation constant of the medium.

The ratio of these quantities define the relative refractive index :

$$m = \frac{k_1}{k_2} \qquad (13)$$

The incident wave is descrided by :

$$E_i = E_0 \exp(-i\omega t) \sum_{n=1}^{\infty} i^n \frac{2n+1}{n(n+1)} \left(m_{01n}^{(1)} - i n_{e1n}^{(1)} \right) \qquad (14)$$

$$H_i = E_0 \frac{k_2}{\mu_2 \omega_2} \exp(-i\omega t) \sum_{n=1}^{\infty} i^n \frac{2n+1}{n(n+1)} \left(m_{e1n}^{(1)} + i n_{o1n}^{(1)} \right) \qquad (15)$$

The equations giving the wave inside the particle, and the scrattered wave are such that :

$$E_r = E_0 \exp(-i\omega t) \sum_{n=1}^{\infty} i^n \frac{2n+1}{n(n+1)} \left(a_i^r m_{01n}^{(3)} - i b_n^r n_{e1n}^{(3)} \right) \qquad (16)$$

$$H_r = -E_0 \frac{k_2}{\mu_2 \omega} \exp(-i\omega t) \sum_{n=1}^{\infty} i^n \frac{2n+1}{n(n+1)} \left(b_n^r m_{e1n}^{(3)} + i a_i^r n_{o1n}^{(3)} \right) \qquad (17)$$

$$E_t = E_0 \exp(-i\omega t) \sum_{n=1}^{\infty} i^n \frac{2n+1}{n(n+1)} \left(a_i^t m_{01n}^{(3)} - i b_n^t n_{e1n}^{(3)} \right) \qquad (18)$$

$$H_t = -E_0 \frac{k_1}{\mu_1 \omega} \exp(-i\omega t) \sum_{n=1}^{\infty} i^n \frac{2n+1}{n(n+1)} \left(b_n^t m_{e1n}^{(3)} + i a_i^t n_{o1n}^{(3)} \right) \qquad (19)$$

where u_1 or u_2 is the magnetic permeability :

$$m_{01n}^{(l)} \;,\; m_{e1n}^{(l)} \;,\; n_{o1n}^{(l)} \;\; and \;\; n_{e1n}^{(l)} \quad with \; l = 1, 3$$

are quantities expressed in terms of *Ricatti - Bessel* functions.

Using the boundary conditions : the tangentiel components of E and H be continous across the spherical partical surface $r = a$, the above equations lead to linear equations in the coefficients a_n^r; b_n^r; a_n^t; b_n^t. Only the first two are of interest here and these are given by :

$$a_n^r = \frac{\Psi_n(\alpha)\Psi_n'(\beta) - m\Psi_n(\beta)\Psi_n'(\alpha)}{\zeta_n(\alpha)\Psi_n'(\beta) - m\Psi_n(\beta)\zeta_n'(\alpha)} \qquad (20)$$

$$b_n^r = \frac{m\Psi_n(\alpha)\Psi_n'(\beta) - \Psi_n(\beta)\Psi_n'(\alpha)}{m\zeta_n(\alpha)\Psi_n'(\beta) - \Psi_n(\beta)\zeta_n'(\alpha)} \qquad (21)$$

where :

$$\beta = k_1 a = ma$$

$$\alpha = k_2 a = \frac{2\pi}{\lambda}$$

$$m = \frac{k_2}{k_1}$$

is the refractive index of the particle relative to that of the medium.

The scattering coefficients a_n^r, b_n^r are expressed in terms of *Ricatti - BESSEL* functions.

2) - Influence of rainfall on radiowave propagation

High frequency microwave systems availability is hampered by certain climatic conditions, mainly heavy rainfall. Maximum allowable path distances are determined by examining the rain cumulative distribution for the given locality.

When it rains in a microwave propagation path, the wave energy flow can be attenuated by the raindrops in the first fresnel zone. Such an attenuation the amplitude of which depends on the wave frequency, the rain temperature , the water index, and the raindrop spectrum results from two phenomena : the absorption and the scattering effects of instantaneous rainfall due to the complex refrative index of the water drops.

The total energy abstracted from the wave beam characterized by the total cross section for the particle comprises the energy abstracted from the incident beam both by scattering and absorption. This is designed as the extinction cross section Q_{ext} and is the sum of the scattering cross section Q_{sca} and the absorption cross section Q_{abs} such that :

$$Q_{ext} = Q_{sca} + Q_{abs} \qquad (22)$$

where:

$$Q_{ext} = \left(\frac{\lambda^2}{2\pi}\right) \sum_{n=1}^{\infty} (2n+1)(|a_n^r|^2 + |b_n^r|^2) \qquad (23)$$

$$Q_{ext} = \left(\frac{\lambda^2}{2\pi}\right) \sum_{n=1}^{\infty} (2n+1)\{R_e(a_n^r + b_n^r)\} \qquad (24)$$

For very small drops such that :

$$\frac{2\pi}{\lambda} \ll 1 \qquad or \qquad \frac{\pi D}{\lambda} \ll 1 \qquad with\ D\ as\ raindrop\ diameter,\ then:$$

$$Q_{sca} = \frac{8}{3} a^4 \left| \frac{m^2 - 1}{m^2 + 2} \right|^2 \qquad (25)$$

$$Q_{abs} = 4\alpha\, Im\left| -\frac{m^2 - 1}{m^2 + 2} \right| \qquad (26)$$

according to rayleigh theory.

In a way that provides a rather intersting physical insight into the above process, *Van de HULST* has shown that if the wave is scattered in a forward direction, the total extinction cross section of the particle is related to the scattering amplitude S (o) by :

$$\sigma_t = \frac{\lambda^2}{\pi a^2} R_e S(o) \qquad (27-a)$$

$$= Q_{ext} \pi a^2 \qquad (27-b)$$

The above quantity being dependent on the drop shape, S (o) is related to the wave polarization : horizontal H, or vertical V.

The specific attenuation per unit length due to rain is then given by :

$$A_{H,V}(dB) = 8.686 \int_{a_{min}}^{a_{max}} \sigma_t(a) N(a) da \qquad (28)$$

Where N(a) da is the raindrop size distribution depending on the rain rate R(mm/h)

OLSEN and *ROGERS* [6] have shown that :

$$A_{H,V}(dB) = k_{H,V} R^{\alpha_{H,V}} \qquad (29)$$

where α, and k are parameter which depend on the frequency and polarization of the radio wave as well as the raindrop spectrum.

The *Laws* and *Parsons* raindrop spectrum and the *Marshall Palmer's* one [5] are the most used to calculate specific rain attenuation. But in fact both laws are appropriate for temperate zones. For tropical zones, *Ajayi* and *Olsen* [7], on the one hand and *Moupfouma* [8] in the other hand have proposed from theoretical work and measurements made respectively in Nigeria and the Congo raindrop spectrum which characterize Tropical and Equatorial zones.

Using the rainfall rate relation such as :

$$R = \frac{4\pi}{3} \int_{a_{min}}^{a_{max}} V(a) N(a) a^3 da \qquad (30)$$

where V(a) is the fall velocity in m/s of a raindrop with radius a such that ; a_{max} and a_{min} are respectively the radius of the largest raindrop and the radius of the smallest. N(a) is their drop size distribution. *Moupfouma* showed that [5] the influence of the drop maximum size is related to the rain rate value :

For 20 mm/h the maximum radius value of the drop is about 3.25 m, since for 150 mm/h this threshold is about 5 mm.

He then concluded that even in tropical and equatorial regions , rain effects on microwave systems are stronger than in other regions due to convective rains. In spite of the presence of raindrops, rain attenuation on high frequency is mainly due to small and mean drops, the number of which in a given rain rate value is more important.

Therefore when integrating eqn (28) for the specific rain attenuation from zero to plus infinity, the error is quite negligible.

The design and the implementation of satellite and terrestrial communication systems involve the knowledge of the propagation parameters which govern link availability service quality.

To derive approximate attenuation statistics for any microwave link, one needs a good prediction method.

Coming back to rain the latter consists of cells and is never uniform on a path. These cells lead to an inhomogeneity of the rainfall on the propagation path, which will be taken into account in the computation of attenuation by introducing a correction coefficient C.

l (km) being the physical radio path length and C the correction coefficient, then we define the effective path length Leq, on which rain is supposed to be uniform now and such that :

$$Leq = C\,l \qquad (31-a)$$

The rain induced attenuation in the propagation path using the above effective path length concept is then :

$$A\,(dB) = \int_0^{Leq}\left(8.686\int_0^{\infty}\sigma_t(a)N(a)da\right)dx \qquad (32-a)$$

$$A\,(dB) = k\,R^{\alpha}\,Leq \qquad (32-b)$$

Recently the author proposed [9] a formula giving correction coefficient such that :

$$C(l,f,R_p,P) = \frac{u(p)\left(\frac{R_{001}}{R_p}\right)^{\alpha(l)}}{1+\eta\left(\frac{P}{0.01}\right)^{-0.36\,l^{m(f,l)}}} \qquad (32-c)$$

where $R_{0.01}$ (mm/h) and R_p (mm/h) represent point rainfall intensities observed on the radio path during 0.01% and P(%) of the time, respectively,P being the same time percentage for which the attenuation exceedance is to be calculated.

3) - Application of the proposed method to L.O.S [9]

For the computation of rain attenuation suffered by a terrestrial radio link, m(f, l) is such that :

$$m(l,f) = 1 + 1.4e-4\times f^{1.76}\,Log_e(l) \qquad (33)$$

where f (GHz) is the radio frequency and l (km) the physical radio path lengh.

Parameters u, v, and η have been determined using the CCIR data and are given for any path :

$$V(l) = 0.38\,l^{-0.25)} \qquad (33)$$

$$\eta = \begin{cases} 0 & \text{if } l<5km \text{ and } f<25GHz \\ 0.03 & \text{in all other cases} \end{cases} \qquad (34)$$

Relation (11) is easily explainable, since a short link (l < 5 km) may be contained almost entirely in a rain cell. Moreover, according to the analysis we carried out, for frequencies lower than 25 GHz, the rain effects observed on radio link with a path length smaller than 5 km, are similar to those due to a uniform rainfall on the whole path considered.

TABLE 4 -Values of parameter u for terrestrial links.

Characteristics of the radio path	Expressions of u (P) as function of P	
	$P \le 0.01$ %	$P > 0.01$ %
l < 5 km and f < 25 GHz	821.4 P^2 - 34.6 P + 1.3	0.93 $e^{4.14P}$
$l \ge$ 50 km with any f (GHz)	0.74 $P^{0.07}$	1.48 $P^{0.105}$
All other cases	0.71 $P^{0.07}$	0.89 $e^{1.6P}$

Unlike the so-called CCIR reduction coefficient [CCIR/338] which is always lower than 1, the correction coefficient proposed in relation (32) is lower than 1 for convective rain with high rain rate, and greater than 1 for stratiform rain. This seems logical [fig 1].

Figures 2 and 3 show that a better agreement is achieved between experimental data gathered in Darmstadt (FRG) and Paris (France) and predicted attenuation derived from our model, rather than with the CCIR model.

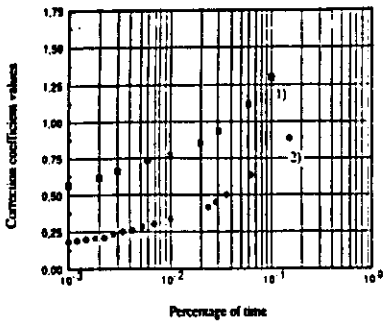

FIG. 1. — Behaviour of the correction coefficient for terrestrial paths.
1) Mendlesham - UK (7.4 km, 19.4 GHz - V).
2) Paris - France (58 km, 11.7 GHz - H).

Comportement du coefficient de correction des trajets terrestres.

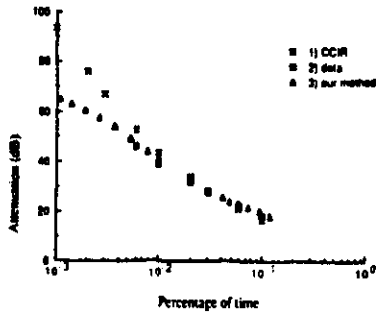

FIG. 2. — Rain attenuation on terrestrial path Darmstadt - TAU (29 GHz, 20 km, H-pol).

Affaiblissement dû à la pluie sur une liaison terrestre.
1) CCIR.
2) Données expérimentales.
3) Notre méthode.

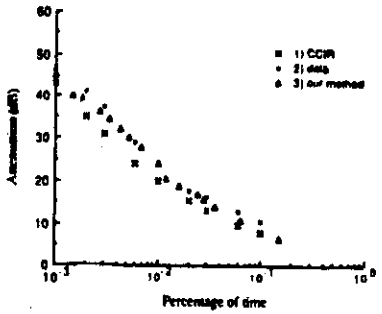

FIG. 3. — Rain attenuation on terrestrial path Paris - France (11.7 GHz, 58 km, H-Pol).

Affaiblissement dû à la pluie sur une liaison terrestre.
1) CCIR.
2) Données expérimentales.
3) Notre méthode.

4) - Application to earth -space path

Calculation of the attenuation on the earth space path is carried out by assuming a uniform rain extending from the ground to an effective height which corresponds to rain height.

II - Concept of vertical rain height for evaluation of rain attenuation on slant paths.

the equivalent path length depends on rain height. The height of the rain top varies with rain structre and with latitude. Thus it cannot be the same in temperate zones as in tropical ones.

CCIR defined the rain height as the mean value of the 0°C isotherm during rainy season, and expressed it as a function of latitude (Reports 563-3, and 564-3) such as :

$$H_R = \begin{cases} 4 & 0 < \phi < 36^\circ \\ 4 - 0.075(\phi - 36) & \phi > 36^\circ \end{cases} \qquad (35)$$

Thus the slant path length L_s is obtained from :

$$L_S = \begin{cases} \dfrac{H_R - H_0}{Sin\theta} & for\ \theta < 5^\circ \\ \dfrac{H_R - H_0}{\left((Sin^2\theta) + 2\dfrac{H_R - H_0}{8500}\right)^{0.5} + sin\theta} & for\ \theta \geq 5^\circ \end{cases} \qquad (36)$$

where θ is the path elevation angle, and H_0 (km) is the station height above mean sea level.

At the present stage,there is no known mathematical relation giving precipation height in equatorial and tropical regions. Some observations of the 0°C isotherm height made in Douala (Cameroon) and Bangui (Central african Republic) during the heaviest rain season are reported in table 1 [10]. They allow precipitation height in tropical regions to be roughly estimated according to the CCIR concept. These isotherm heights appear to be higher than those given by CCIR for low latitudes; so they cannot allow the rain attenuations to be reduced.

Height of 0°C isotherm in Douala during July 1980						
Date	3	6	10	15	19	21
Height (m)	4600	5030	4700	5070	4600	4400
Pressure mb)	584	556	578	563	580	590

Table 5- a : heights of 0°C isotherm in some african tropical localities.

Height of 0°C isotherm in Bangui during July 1980				
Date	2	10	18	26
Height (m)	4900	4600	4900	4650
Pressure mb)	555	570	550	550

Table 5- b : heights of 0°C isotherm in some african tropical localities.

Therefore, the concept of 0°C isotherm to determine the rain height as proposed by CCIR is not a good one for solving the problem posed by low latitude localities.

CCIR should work at finding for the rain height, a better definition, and perhaps a new expression which would incorporate new parameters in the calculation of rain attenuation.

Attenuation on Earth-space paths will be estimated here by an extension of the rain attenuation prediction method for terrestrial paths. The terrestrial pysical path length l (km) is now replaced by the slant path length L_s given by eqn. (36). THus the predicted rain attenuation on a satellite link can be obtained from :

$$A_p(dB) = kR_p^{\alpha} \frac{u(p)\left(\frac{R_{001}}{R_p}\right)^{0.38 L_s^{-0.25}}}{1+\eta\left(\frac{P}{0.01}\right)^{-0.36 f^{m(f,l)}}} L_S \qquad (37)$$

with

$$m(L_s f) = 1 + 1.4e{-}4 \times f^{1.76} Log_e(L_s) \qquad (38)$$

Parameter η is given by eqn (34) as a function of L_s rather than l (km).Values of parameter are listed in table 6.

Regions	Parameter u for slant paths as a function of time percentage P(%)	
	$L_s \geq 5$ km	$L_s \leq 5$ km
Australia	$u = 0.24\ P^{0.13}$	$u = 0.47\ P^{0.02}$
Europe	$u = 1.11\ P^{0.035}$	$u = -38\ P^2 + 7P + 0.65$
Japan	$u = 1.54\ P^2 - 1.3\ P + 0.9$	$u = 1.73\ P^{0.12}$
USA	$u = -0.3\ P^2 - 0.007P + 0.82$	$u = 1.3\ P^{0.06}$

Figures on which experimental data gathered in several countries are compared to calculated attenuation from the above model can be seen in [9]

Reference

1 - *Moupfouma F.*: "More about rainfall rates and their prediction for radio system engineering". IEE proceedings, vol.134, Pt. H, No.6, Dec.1987 pp 527-537

2 - *CCIR* XV th plen.Ass, Dubrovnik, 1986-V, Report 563-3

3 - *Moupfouma F.*: "Model of rainfall rate distribution for system design," IEE proceedings, vol.132 (1), Pt. H, No.6, Dec. 1985 pp. 39-41

4 - *Moupfouma F.*:"Atlas mondial des intensités de pluie integrées sur 1 min pour les études de faisabilité de liaisons hertziennes et par satellite," Note tech. T/LAB/MER/219 - NT/PAB/RPE/149, 1986

5 - *Moupfouma F.*"Etude des précipitations et de leurs effets sur les liaisons hertziennes en visibilité et par satellite dans les régions tropicales", Thèse de Doctorat d'ETAT 1987 CNET/Paris

6 - *Olsen (R.L.), Rogers (D.V.), Hodge (D.B.)* The aR^b relation in the calculation of rain attenuation. IEEE trans. AP, USA (1978), 26, pp. 318-329

7 - *Ajayi G.O., Olsen (R.L.)*, "Modeling of a tropical raindrop size distribution for microwave and millimeter wave applications," Radio science, vol. 20, n°2, pp 193-202, April 1985

8 - *Moupfouma F.*, and *Tiffon,J.*:"Raindrop size distribution from microwave scattering measurements in equatorial and tropical climates," Elect. letters, vol. 18, n°23, pp. 1112-1113, Nov. 1982

9 - *Moupfouma F.*,:"Rain induced attenuation prediction model for terrestrial and satellite - earth microwave links," Annales des Télécommunications, tome 42, n°9 - 10, septembre - octobre 1987 pp. 539- 550

10 - *Moupfouma F.*, and *Spanjaard ,N.*:"Rain effects on microwave communications in Equatorial and tropical region." IEEE Global Telecommunications Conference (GLOBECOM) Dec.1 - 4, 1986, pp. 197 - 201.

PROPAGATION IN IONIZED MEDIA

1 - Introduction

The ionosphere may be defined as the region extending from about 50 km to roughly 2000km above the earth's surface. It is divided into three layers designed D, E, F respectively in order of increasing altitude.

The D region streches from 50 to 90 km and acts as an absorber, causing HF wave attenuation, although VLF and ELF at those altitudes.

The E layer with altitude ranging from 90 to 130 km, and the F one extending upward from about 130 km act principally as radio reflector which permit long range propagation between terrestrial terminals.

The term ionosphere was coined by *WATSON - WATT* in 1926 [1]. Nevertheless due to his transatlantic radio transmission system, *MARCONI* discovered earlier in 1901 this part of the atmosphere in which free electrons are sufficiently numerous to influence the propagation of radiowaves.

2 - Ionospheric effects.

The principal source of ionization in the ionosphere is electromagnetic radiation from the sun extending over the ultra violet and X- ray portions of the spectrum. The sun's radiation being progressively absorved when passing through the atmosphere, its residual ionizing ability depends upon the length of the atmospheric path.

The maximum ionization rate occurs when the sun is at solar zenith. Below 60 km altitude, galactic cosmic rays constitute the dominant source of ionization.

Considering such medium rendered anisotropic by the presence of the earth's magnetic field, the concept of characteristic waves that propagate in it is important. These are waves which propagate without changing their polarization.

The characteristics of such waves depend upon the direction of propagation with respect to earth magnetic field as shown in fig.1 :

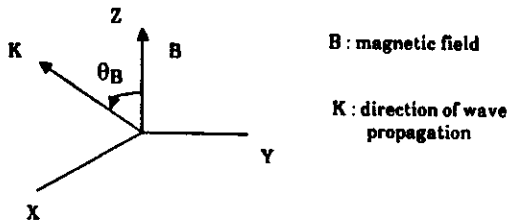

B : magnetic field

K : direction of wave propagation

Fig. 1

3 - Parallel propagation

There are two characteristic waves. When the propagation is parallel to the magnetic field B (see fig.1), the two characteristic waves are left and right circularly polarized and are characterized by index of refraction n_l and n_r such as :

$$n_l^2 = k_l = 1 - \frac{w_p^2}{w(w + w_B)} \qquad (1)$$

and

$$n_r^2 = k_l r = 1 - \frac{w_p^2}{w(w - w_B)} \qquad (2)$$

k_l and k_r are the relative dielectric constant for the left and the right circularly polarized waves. w is the angular plasma frequency of the wave such that

$$w = 2\pi f_{Hz} \qquad (3)$$

$$w_p^2 = \frac{eB}{m} \qquad (4)$$

with m=9.1096e-31kg as its mass and e=1.6022e-19C as its charge. B is expressed in wb/m^2.

The quantity w_p^2 is the angular plasma frequency such that :

$$w_p = \frac{Ne^2}{m\varepsilon_0} \qquad (5)$$

N is the electron density (el/m3) and ε_0 the electric permittivity of empty space (8.854 e-12 F/m).

A right circularly polarized wave has an electric field intensity vector of constant length that rotates with angular velocity w in the circular direction, which can be defined by the direction of the fingers of the right hand. A left circularly polarized wave rotates in opposite direction.

4 - Perpendicular Propagation.

For propagation perpendicular to the magnetic field, one characteristic wave has its electric field intensity vector directed along the Z axis. The electric field E in this case imparts a velocity to the free electrons in the Z direction, with the result that the electrons are unaffected by the magnetic field, as no magnetic force is exerced on charged particles having velocities parallel to the magnetic field.

The refractive index n_o for this case is given by :

$$n_0^2 = 1 - \frac{\omega_p^2}{\omega^2} \qquad (6)$$

The index o means that this wave is referred to as ordinary wave because it is unaffected by the magnetic field.

5 - Reflection effects

Coming back to equation (6), it appears that for $w > w_p$, the refractive index n_o is real; but for $w < w_p$, n_o is imaginary

While the propagation constant k is related to the constitutive constants of the medium by :

$$k^2 = \mu\varepsilon\omega^2 - j\mu\sigma\omega \qquad (7)$$

and may be represented as :

$$k = \alpha - j\beta \qquad (8)$$

with

$$\alpha = \omega\left[\frac{\mu\varepsilon}{2}\left[\left(1+\frac{\sigma^2}{(\varepsilon\omega)^2}\right)^{0.5}+1\right]\right]^{0.5} \qquad (9)$$

$$\beta = \omega\left[\frac{\mu\varepsilon}{2}\left[\left(1+\frac{\sigma^2}{(\varepsilon\omega)^2}\right)^{0.5}-1\right]\right]^{0.5} \qquad (10)$$

when the refractive index is imaginary $w < w_p$ thus an electromagnetic wave propagating along the positive Z axis described by :

$$E = E_o \exp j(\omega t - kz) \qquad (11)$$

becomes

$$E = E_o \exp(j\omega t - \beta z) \qquad (12)$$

$\exp(-\beta z)$ provides for the damping of the wave as it progresses in the z direction and corresponds to the absorption of part of the radiant energy.

$E_o\exp(-\beta z)$ represents a field that attenuates with z

If $w > w_p$ then the ray path is unaffected by the ionosphere as shown in fig 2-a

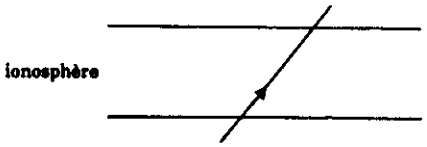

Fig 2-a

If $w < w_p$ in the vertical path, the ray is reflected (fig 2-b).

Fig 2-b

Within each region of the ionosphere exist one or more layers of ionization distinguished by symbols F1; F2; Es. Propagation conditions in those layers largely depend on the peak electron densities NmE, NmF1 and NmF2 of layers related to the penetration frequencies at vertical incidence foE, foF1, foF2.

The ionosphere shows a great deal of variability. The F2 layer is the most variable, since the E-layer is the least variable.

6-The Faraday rotation

The basis of Faraday rotation for a linearly polarized high frequency wave propagating through the ionosphere is that a linearly polarized wave consists of left and circularly polarized components which have different indices of refraction.

Let E_l and E_r be the electric field intensity vectors of left and right circularly polarized waves. As these vectors propagate in the Z direction they continue to rotate with angular velocity w in their respective directions. Fig.3 shows a possible condition after propagation through some distance z namely rotation of E through an angle ϕ in the right direction. such as

$$\phi = \frac{\beta_l Z - \beta_r Z}{2} \qquad (13)$$

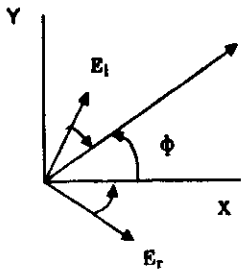

Fig. 3

For frequencies sufficiently high, the total rotation ϕ in radian along the path is given by :

$$\phi = \frac{e^3}{8C\varepsilon_o m^2 n^2 f^2} \int NB\cos\theta_B \, dl \qquad (14)$$

Setting

$$B_L = \frac{\int NB\cos\theta_B \, dl}{\int N \, dl} \qquad (15)$$

then

$$\phi = \frac{2.36\,10^4}{f^2} B_L \int N \, dl \qquad (16)$$

or else

$$\phi = \frac{2.36\,10^6}{f^2} B_L TEC \qquad (17)$$

where TEC is the total electron content (TEC) in m^{-2} such as :

$$TEC = \frac{\phi f^2}{2.36 \times 10^6 B_L} \qquad (18)$$

on a fixed path, the amount of Faraday rotation depends on the TEC which exhibits a pronounced variation with season and diurnal variations.

The use of sufficiently high frequency makes the Faraday rotation negligible.

n being the refractive index and N (el / m^3) the electron density ,for frequencies higher than 100 Mhz, when neglecting refraction, then :

$$n^2 = 1 - \frac{80.6\,N}{f^2} \quad if \quad n \neq 1 \qquad (19)$$

$$Since \quad \frac{80.6\,N}{f^2} < 1 \qquad (20)$$

$$Then \quad n \approx 1 - \frac{40.3\,N}{f^2} \qquad (21)$$

$$Setting \quad \frac{d\Delta\varepsilon}{dl} = 1 - n \qquad (22)$$

when $\Delta\varepsilon$ represents a positive error on the path, then :

$$\Delta\varepsilon = \int (1-n)\, dl \approx \frac{40.3}{f^2} \int N \, dl \qquad (23)$$

$$with \quad \int N \, dl = TEC \qquad (24)$$

TEC being the total electron content along the path

$$Thus \quad \Delta\varepsilon \approx \frac{40.3}{f^2} TEC \qquad (25)$$

Using the phase constant β such as :

$$\beta = \frac{2\pi}{\lambda} = \frac{2\pi}{c} f \qquad (26)$$

with C as the wave velocity in the vacum, then :

$$\Delta\varepsilon\beta \approx \Delta\phi = \frac{8.44 \times 10^{-7}}{f^2} TEC \qquad (rad) \qquad (27)$$

$\Delta\phi$ is the phase advance. The presence of the ionosphere actually advance the phase of a received signal with respect to the value for the propagation through the unionized air.

The frequency and the phase being related such as :

$$2\pi f = \omega = \frac{\Delta\phi}{\Delta t} = \qquad (28)$$

then the doppler shift in frequency f_D corresponding to the phase change $\Delta\phi$ can be defined such as :

$$f_D = \frac{8.44 \times 10^{-7}}{\Delta\phi} \times TEC \qquad (29)$$

The electron content of the ionosphere shows a pronounced diurnal variation consistent with the production of ionization by solar radiation in the day time and the decay of ionization at night.

Fig. 4 gives curves showing the diurnal variation of TEC for an invariant latitude of 54°.

Fig. 4 Diurnal variations in TEC, mean monthly curves for 1967 to 1973 as obtained at Sagamore hill, MA using 136 MHz signals from ATS-3 (after Hawkins and Klobuchar, 1974).[2]

IONOSPHERIC ABSORPTION AND SCINTILLATION.

Scintillations are irregular variations of signals. *Hewish* (1952) [3] attributed them to a diffraction pattern formed at the ground by a drifting pattern of irregularities in the ionosphere at a high altitude (about 400km). More *Aarons and al* (1971) showed that these irregularities are mostly in the F layer above about 230 to 400 km

Due to the coming of satellite it was seen that the scintillation occurs at frequencies at least as high as 6 Ghz with significant scintillation at 4 and 6 Ghz in equatorial latitudes

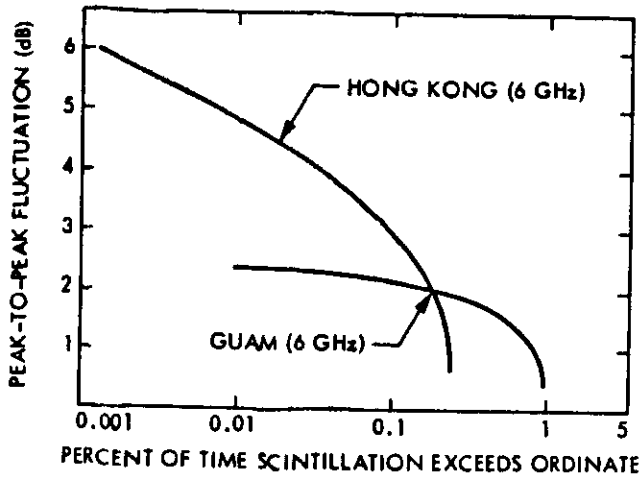

Fig. 5 Scintillation, Guam and Hong Kong (Taur, 1973)[1]

Theoretical aspects

Let us consider a path of length d between transmeting and receiving locations. At distances d_T and d_R from the transmitter and the receiver, the first Fresnel zone radius F1 is given by :

$$F_1 = \sqrt{\frac{\lambda d_T d_R}{d}} \qquad (30)$$

All the elements of radiation passing through the first Fresnel zone have components of electric field intensity that add constructively.

If d_T approches d, that means it becomes very large, then :

$$F_1 = \sqrt{\lambda d_R} \qquad (31)$$

The first Fresnel zone being circular in cross section, considering irregularities that occur with a radius or scale size L about equal to F1 at height h = z above a point of observation, then equation (30) becomes :

$$L = \sqrt{\lambda z} \qquad (32)$$

To analyse scintillation, a model involving diffraction in an ionospheric screen has been widely employed. Meanwhile this model is suitable if only the irregularities are confined to a suffisciently thin layer.

The *Rytov* approximation based upon a solution of the scalar wave equation as given by equation (33) (*Tatarski* 1971) [5], provides a mean of treating the general case

$$(\nabla^2 + k_0^2 n^2)\, u(r) = 0 \qquad (33)$$

u(r) represents a component of electric field, n the refractive index, and $k_0 = 2\pi/\lambda$.

A solution of equation (32) can be obtained by setting :

$$u(r) = u_0(r) \exp(\psi_1(r)) \qquad (34)$$

$$\text{with} \quad \psi_1(r) = \log_e \frac{A}{A_0} + j(S - S_0) \qquad (35)$$

where S is the phase fluctuation.

Note that the *Rytov* approximation doesn't always correctly predict observed scintillation characteristics.

Equatorial scintillation is often characterized by a sudden onset and its occurence varies considerably with location within the equatorial region.

Scintillation tends to be most intense in equatorial, auroral, and polar latitudes as one can see on table 1 (ccir1978)

Table 1. Percentage of occurrenceof scintillation (CCIR, 1978).

(a) > 10 dB peak to peak, equatorial latitudes

Site	Frequency	Day	Night
		(0400-1600 LT)	(1600-0400 LT)
Huancayo (Peru)	137 MHz	3	14
	254 MHz	2	7
		(0600-1800)	(1800-0600 LT)
Accra (Ghana)	137 Mhz	0.4	14

(b) > 12 dB peak to peak at 137 MHz, sub-auroral and auroral latitudes

Site	K_p	Day (0500-1700 LT)	Night (1700-0500 LT)
Sagamore Hill (Massachusetts)	0 to 3+	0	1.4
	> 3+	0.1	2
Goose Bay (Labrador)	0 to 3+	0.1	1.8
	> 3+	1.6	6.8
Narssarssuaq (Greenland)	0 to 3+	2.9	18
	> 3+	19	45

(c) > 10 dB peak to peak at 254 MHz, auroral latitudes

Site	K_p	Day (0600-1800 LT)	Night (1800-0600 LT)
Goose Bay (Labrador)	0 to 3+	0.1	0.1
	> 3+	0.3	1.2
Narssarssuaq (Greenland)	0 to 3+	0.1	0.9
	> 3+	2.6	8.4

LT: Local time.

.Scintillation occurs after sunset and before midnight (fig. 6)

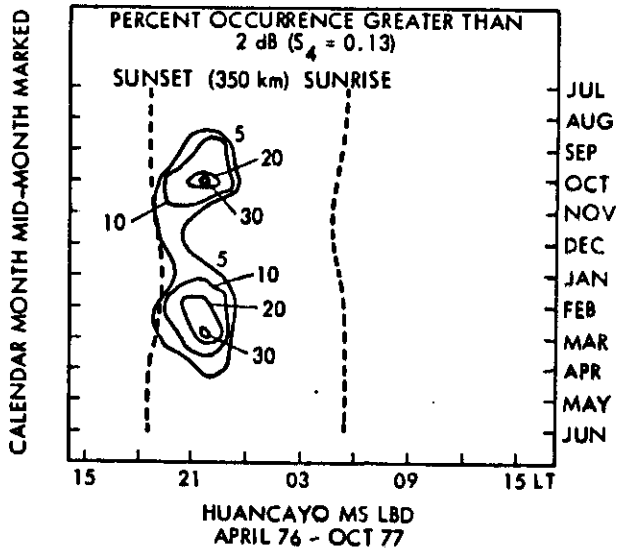

Fig. 6 Monthly precentage occurrence of scintillations ≧ 2 dB, Huancayo, MARISAT, 1.54 GHz. (Basu et a1., 1980)[1].

Amplitude scintillation results in a reduction of signal to noise report in a microwave signal. The phase scintillation may or not be important, depending on the type of system.For digital systems, phase scintillations are unimportant if the bite rate is much greater than the scintillation rate.

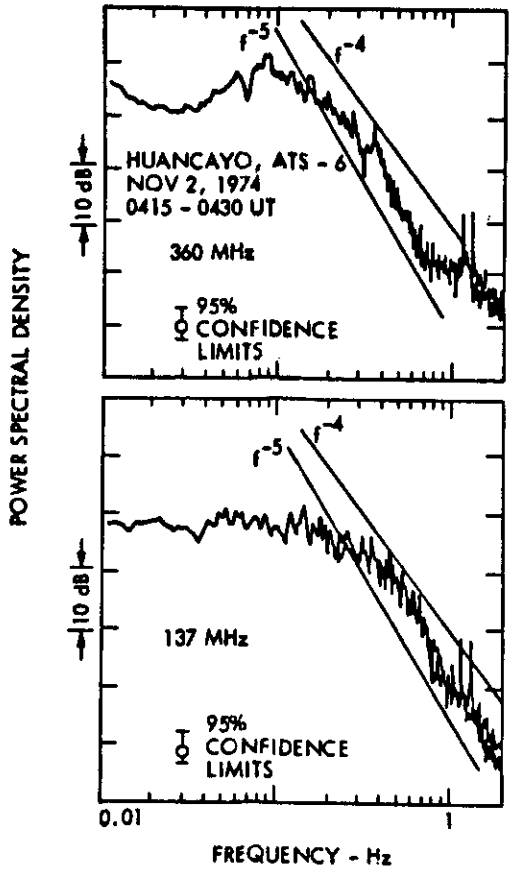

Fig. 7 Typical power spectra for intense scintillations; S_4 = 0.94 at 137 MHz, S_4 = 0.78 at 360 MHz (Whitney and Basu, 1977) [6]

Absorption

The collision of free electrons with neutral atoms and molecules leads to wave attenuation in plasma.

For frequencies above about 30 Mhz the attenuation is such that :

$$A\,(dB/Km) = 8.686 \times a \qquad (36)$$

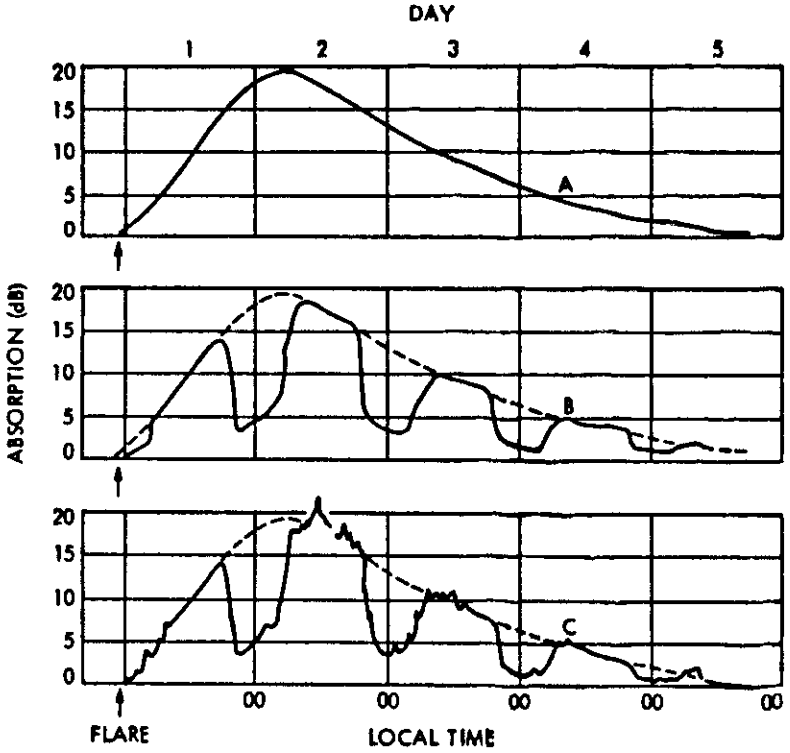

Fig . 8 Model showing polarcap absorption (30 MHz) (CCIR, 1978).
A : High altitudes, 24 hours of daylight.
B : High altitudes, equal periods of day and night
C : Auroral zone

$$With \quad a = \frac{Nq^2\nu}{2\,m\varepsilon_0\,n\,cw^2} \quad Nepers/m \qquad (37)$$

For slant paths, total attenuation is proportional to $\sec\theta / f^2$ where θ is the zenith angle

References

1 - *Warren L. Flock* "Propagation Effects on satellite systems at frequencies below 10 GHz" NASA communication division ref.1108 1983

2 - *Hawkins, G.S.* et *al* : "Seasonal and diurnal variations in the total electron ccontent of the ionosphere at invariant latitude 54 degrees," AFCLR - TR - 74 - 0294. Bedford, Ma : Force Cambrigde Research Labs., 28 June, 1974

3 - *Hewish, A.*: "The diffraction of galactic radio waves as a method of investigating....," Proc. Royal Society of London, Series A, vol. 214, pp. 494 - 514, 9 Octob.,1952

4 - *Aarons* et *al,*: "Global morphology of ionospheric scintillations," Proc. IEEE, vol. 59, pp. 159 - 172, Feb. 1971

5 - *Tatarski, V.E.*: "The effects of the turbulent atmosphere on wave propagation," Springfield, VA : NTIS U.S Depart. of Commerce

6 - *Whitney, H. E.* and *S. Basu*, "The effect of ionospheric scintillation on VHF/UHF satellite communication," Radio science, vol. 12, pp. 123 - 133, Jan. - .1977

7 - *Bean, B. R. and E. J. Dutton*, Radio Meteorology. Washington, DC : Supt. of Documents, U.S. Government Printing Office, 1966

TROPOSPHERIC CLEAR AIR EFFECTS

Refractive index profile

Propagation of radio waves in VHF, UHF and SHF bands is influenced and some cases strongly affected by the variations of meteorological parameters, among which the refractive index n.

The refractive index in a given medium is related to the radio refractivity N at radio frequencies such as :

$$N=(n-1)\times 10^6 = \frac{77.6}{T}\left(P+4810\times\frac{e}{T}\right) \qquad (1)$$

$$N=(n-1)\times 10^6 = \frac{77.6}{T}P+3.75\times 10^5\times\frac{e}{T^2} \qquad (2)$$

with :P as the pressure of dry nonpolar air in mb(millibars)

e as vapor pressure in mb

T as the absolute temperature in Kelvin

Because the index n is only slightly greater than 1, the usual practice is to use N units.

The two terms of equation (2) represent respectively the "dry" and "wet" terms in the refractivity N

The absolute humidity or water vapor density in gm /m^3 ρ, and the vapor pressure are related such as :

$$\rho = 216.8\times\frac{e}{T} \qquad (3)$$

Height dependency

Pressure, temperature, and vapor content decrease with height above the earth's surface in the troposphere on the average, but temperature increases with height in temperature inversion layers.

The atmospheric pressure p(h) depends according to the barometric height formula on the height h, measured in meters above ground such as :

$$p(h) = p(h_o)\exp(-(h-h_o)/C_H) \qquad (4)$$

where ho is the ground height p(h_o) the atmospheric pressure with C_H such as :

$$C_H = 29.66\, m\,(T/K) \qquad (5)$$

The influence of the temperature on the pressure is very small: The error on N is less than 1%, that means, the altitude of the balloon can be evaluated by the inverse function of equation (4).

The atmospheric pressure and the related humidity can be measured simultaneously with collectors, so related humidity and vapor pressure can be determined.

Reference atmosphere

In normal atmospheric conditions, the refractivity decrease with the height above sea level. "A reference atmosphere" is defined by the ccir recommendation 369 / 1. as :

$$N(h) = N_A \exp(-b_A h) \qquad (6)$$

where N_A = 315 N-units as the averaged value at the surface of the earth. and

b_A = 0.136 km^{-1}

The refractivity N_S at the surface of the earth which has the height hs above sea level, can be transformed to the sea level by the use of eq- (6)

$$N_S = N_o \exp(-b_A h_S) \qquad (7)$$

where N_o is the refractivity transformed to sea level as :

$$\Delta N = N_S - N \qquad (8)$$

The exponential model is widely applicable but any reliable data on actual refractivity profiles should be used when available. Such data can be acquired by use of radio sondes or microwave refractometers and often display significant departures from the exponential form.

A common cause of non-exponential refractivity profiles is the occurence of temperature inversion layers.

Refraction and fading

Due to the variation of the refractivity depending on the height, the electromagnetic waves do not travel in straight lines in the troposphere, but experience bending over the earth or refraction. *Bean and Dutton* [1] define the curvature C of the ray path which represent path along which energy is retransmitted such as :

$$C = -\frac{1}{n}\frac{dn}{dh}\cos\beta \qquad (9)$$

with β as the angle of the ray measured from the horizontal.

In order to compensate this bending of ray waves, an effective earth radius ka with "a" as the true earth radius is introduced. The factor k which is known as the effective earth radius factor enhances the real earth radius and can be defined as :

$$\left(\frac{1}{a}+\frac{dn}{dh}\right)=\frac{1}{k R_e} \qquad (10)$$

$$\text{then} \quad k=\frac{1}{\left(1+\frac{a dN}{dh}\right)} \qquad (11)$$

Table 1 lists corresponding values of k and dN/dh.

Table 1 corresponding values of k and dN / dh

$\frac{dN}{dh}$ (N / km)	k
157	0.5
78	2/3
0	1
- 40	4/3
- 100	2.75
- 157	∞
- 200	- 3.66
- 300	- 1.09

The parameters N and k are used to distinguish between different types of refraction (see fig.1).

- Subrefractiive	dN/dh < 40	0<k<4/3
- Reference atmosphere	dN/dh = 40	k=4/3
- Superrefractive	157 > dN/dh > 40	k>4/3
- Ducting	dN/dh≥157	k≤0

The effects of the various k values are illustrated in fig.1 and fig.2. In the first one all the rays are horizontal at the common point. In the second one, ray paths which are shown allow signals from common transmitter to reach a common receiving location.

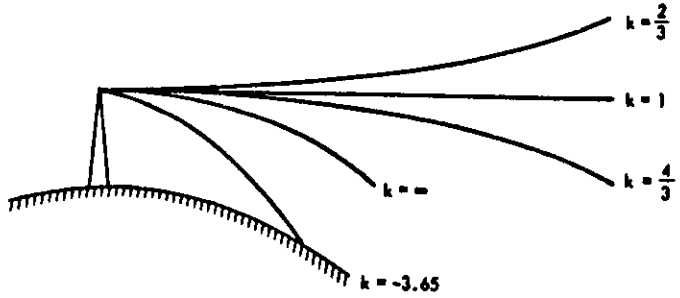

Fig. 1 Ray paths for initially horizontal rays

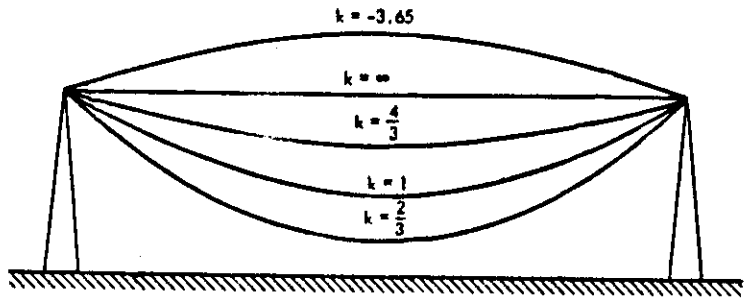

Fig. 2 Ray paths from a transmitter to a receiver

On average, surface refractivity in the equatorial region is higher than in the middle latitude. In Nigeria, it has been noticed that average values for the year decrease from South to North. These are 375, 350, and 375. A high effect characterized by highest values of Ns in coastal localities is noticed in latitude below 20 [2] .

Anomalies of the atmosphere are caused by layers with different refractivity profile. The resulting propagation phenomena are multipath propagation, ducting and defocussing. All those anomalies likely occur only in calm atmosphere.

In order to simplify the treatment of bent radio waves over a spherical earth, one introduces the refractive modulus M(h) defined such as :

$$M(h) = N(h) + 157\, h/km \qquad (12)$$

Ducting may occurs depending on the radio wave length and duct thickness . It can cause radio interference between neighbouring transmission links.

Dougherty et al [2] have found from several year observations, seasonal effect in the refractivity gradient. Using several radio refractivity data from several african countries (Central African Republic, Senegal, Chad, Côte d'Ivoire, Niger...) for several years, *Owolabi and Ajayi* [2] noticed an average high surface ducting occurrence probability of 43 % for the three stations north of latitude 12° N compared with the corresponding probability of 8% for the three stations south of latitude 12° N.

Refractivity investigations were performed in Senegal by *Hautefeuille and Boyle* [3]. They observed very deep fading of up to 50 dB on a 7 GHz Thiès- Koalack - Ziguinchor radio link confirming that the refractivity gradient in West Africa differs strongly from that in Europe, and varies strongly.

The multipath is characterized by energy reaching the receiver of telecommunication system by more than one path. The signals arriving over the different paths tend to arrive with variable relative phase, with the result that they alternatively reinforce each other and interfere destructively. The total signal is then characterized by fading involving repeated minima, and this minima can fall below the acceptable signal.

ITU and CCIR measurement campaign in african countries

As pointed above, atmospheric anomalies are related to climate characteristics. Nevertheless, propagation curves and formula derived from measurements made in Europe are used up to now for planning of radio and telecommunication services for tropical countries, due to the lack of sufficient propagation investigations in this part of the world. As a result of WARC (Geneva-1979) and the ccir-seminar in Lome (Togo), 1982, ITU initiated the radio propagation campaign in some african countries : Burkina-Fasso, Cameroun, Congo. with the support of some Research institutes as "Centre National d'Etudes des Telécommunications (France-TELECOM), Rutherford Appelton Laboratory (UK), the Research Institute of theDeutsche Bundespost (FRG), Intelsat, Comsat (USA).

As ducting and superrefraction are concerned data gathered in Burkina Faso are given here in annexe [4].

References

1 - *Warren L. Flock* "Propagation Effects on satellite systems at frequencies below 10 GHz" NASA communication division ref. 1108 1983

2 - *Oyinloye J., O.* "Characteristics of non-ionized media and radiowave propagation in equatorial areas - A review," Telecomunication journal- vol, 55-11/1988, pp 115-129

3 - *Hautefeuille, M. ; Boyle, A. ; Timmers, a. w.; Shannon, J.D.* : "Evanoissement par propagation guidée....." Journal des Telécommunications, vol. 47 (1980), pp. 517-525

4 - *UIT.* "Campagne de mesures de propagation radioélectrique en Afrique"- Rapport de la réunion d'évaluation. Genève, 17-18 Fevrier 1987

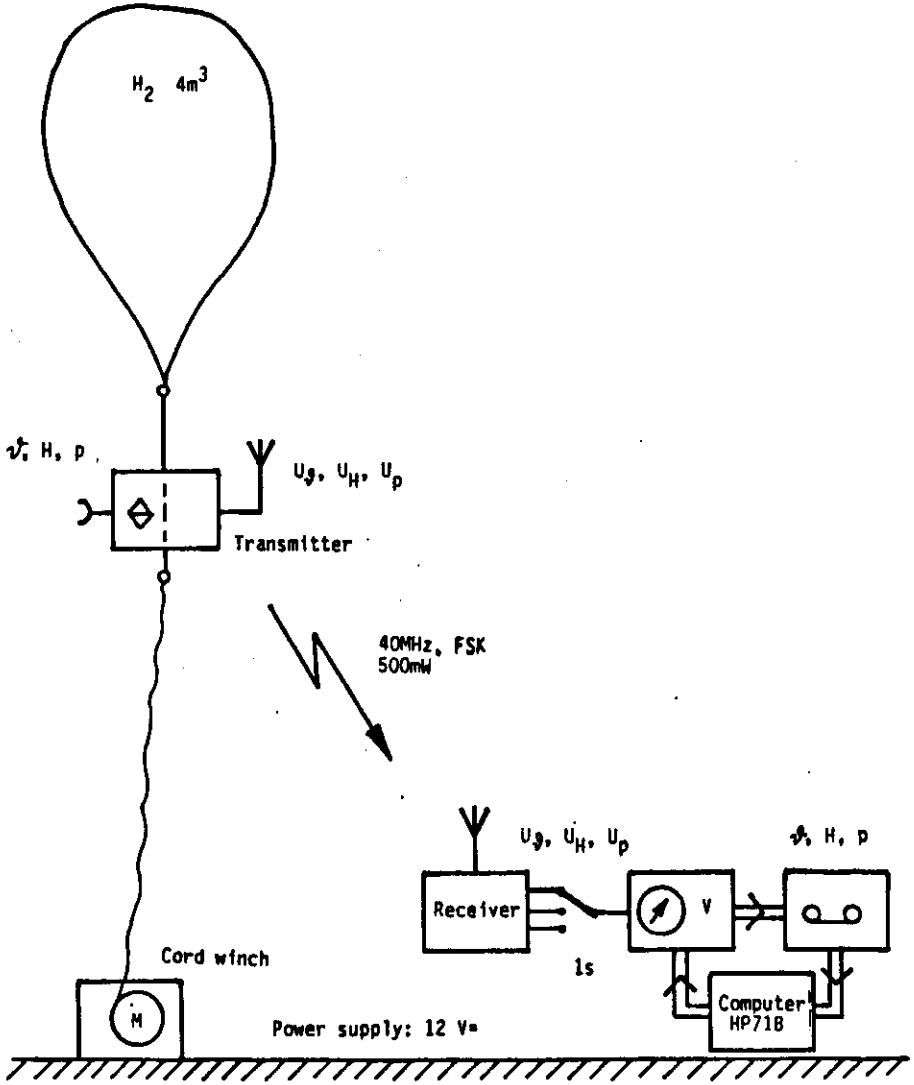

Fig. : Block diagram for the measurement of the temperature, relative humidity and atmospheric pressure with the aid of a balloon.

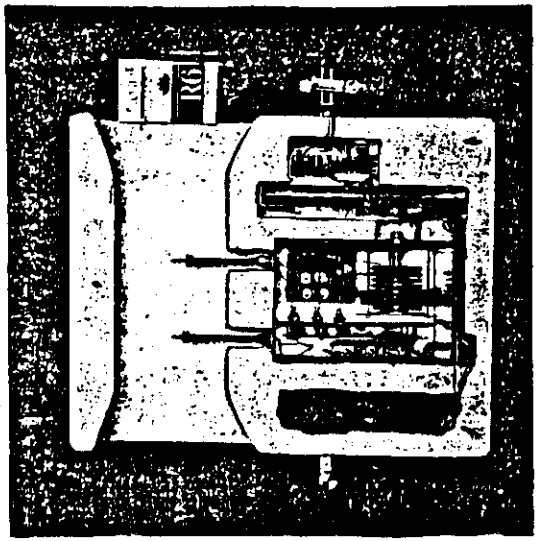

Fig. : Balloon measurement equipment opened.

'ig. : Preparation for a balloon climb.

Fig. : Height profiles of measurement Nr. 1 at 16.10.86, 16.30 h.
a) Temperature versus height.
b) Relative humidity and water vapour pressure vs height.
c) Refractivity and refractive modulus versus height.
The reference atmosphere is indicated by the dashed lines.

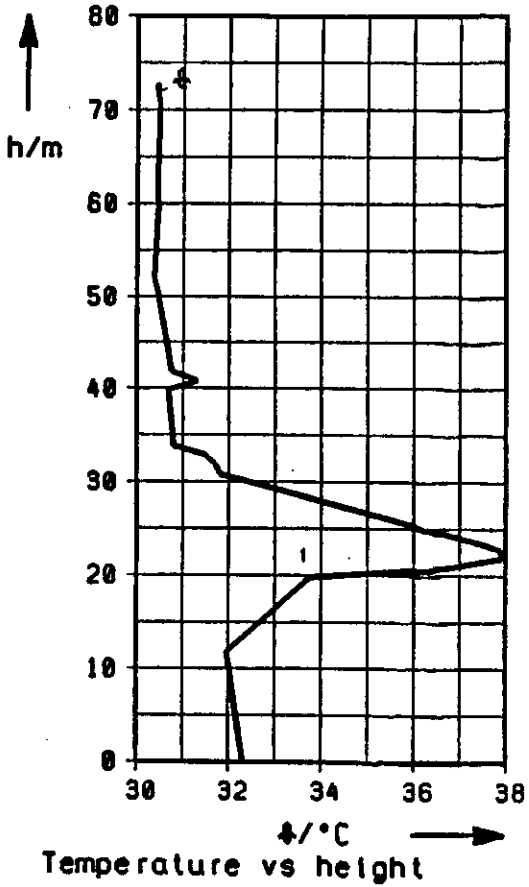

a)

Location:	BOBO-DIOULASSO, AIRPORT
Country:	Burkina Faso
Height:	460 m above sea level
Day:	16.10.1986
Time:	16:30 h Meas.Nr. 1

Fig. : Height profiles of measurement Nr. 2 at 16.10.86, 16.51 h.
a) Temperature versus height.
b) Relative humidity and water vapour pressure vs height.
c) Refractivity and refractive modulus versus height.
The reference atmosphere is indicated by the dashed lines.

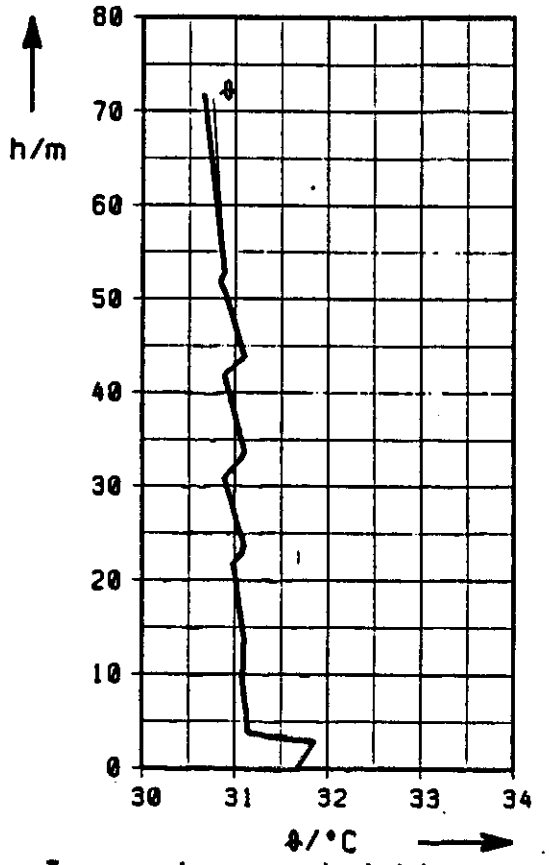

a)

Location:	BOBO-DIOULASSO, AIRPORT
Country:	Burkina Faso
Height:	460 m above sea level
Day:	16.10.1986
Time:	16:51 h Meas.Nr. 2

Water vapour pressure vs height

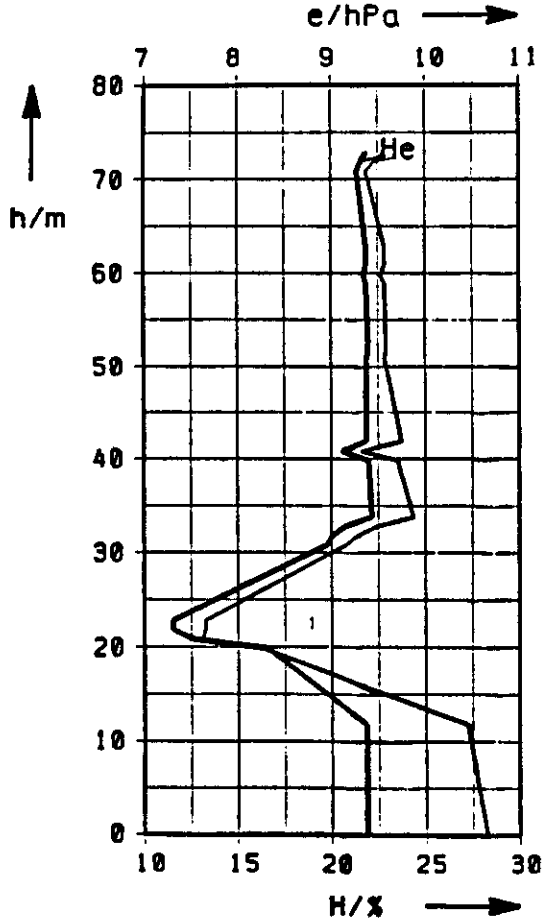

Relative humidity vs height

Location:	BOBO-DIOULASSO, AIRPORT
Country:	Burkina Faso
Height:	460 m above sea level
Day:	16.10.1986
Time:	16:30 h Meas.Nr. 1

G)

Refractive modulus vs height

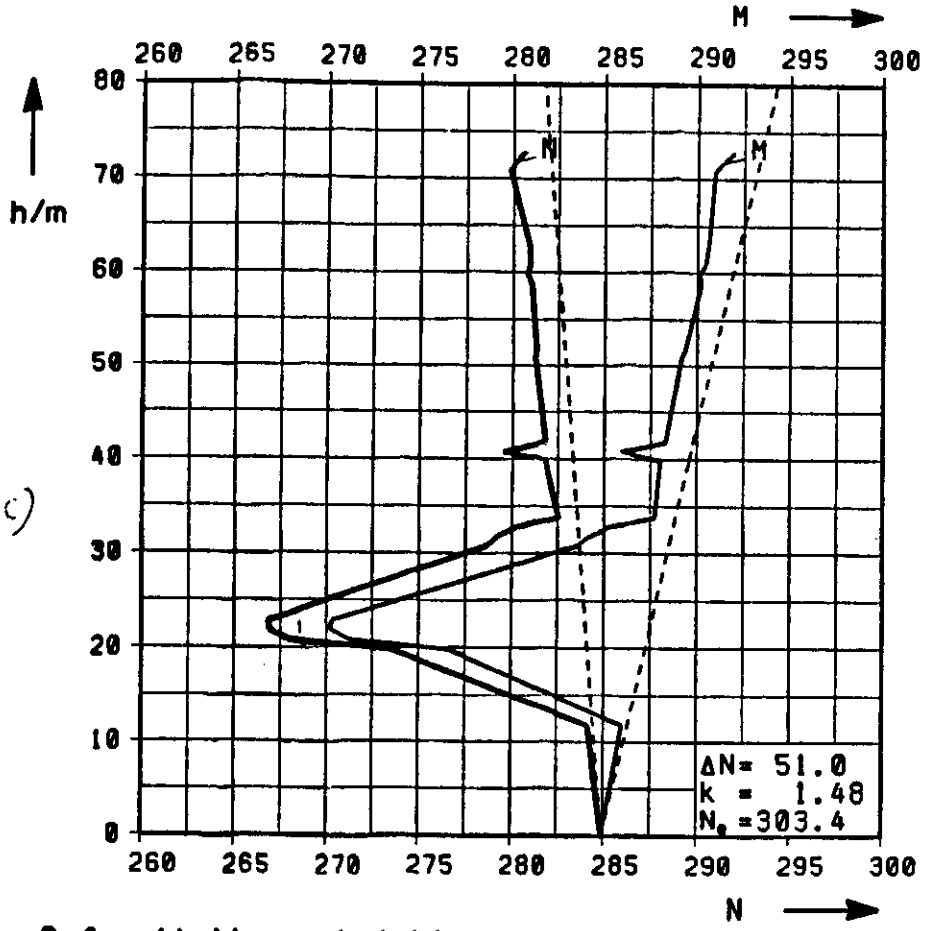

c)

Refractivity vs height

Location:	BOBO-DIOULASSO, AIRPORT
Country:	Burkina Faso
Height:	460 m above sea level
Day:	16.10.1986
Time:	16:30 h Meas.Nr. 1